

OPTICAL PROPERTIES OF ZINC-BOROTELLURITE DOPED SAMARIUM

S.S. HAJER, M. K. HALIMAH*, Z.AZMI, M.N. AZLAN

Physics Department, Faculty of Science, Universiti Putra Malaysia, 43400 UPM Serdang, Selangor, Malaysia.

Glasses with chemical compositional $\{[(\text{TeO}_2)_{0.7}(\text{B}_2\text{O}_3)_{0.3}]_{0.7} [\text{ZnO}]_{0.3}\}_{1-x} \{\text{Sm}_2\text{O}_3\}_x$, (where $x=0, 0.005, 0.01, 0.02, 0.03, 0.04, 0.05$ mol %); were prepared by conventional melt-quenching technique. The structural properties of the prepared glasses were determined by X-ray diffraction (XRD) analysis and FTIR analysis. It was confirmed that the prepared glasses are amorphous. The bonding parameters of the glasses were analyzed by using FTIR analysis and were confirmed to be ionic in nature. The density, molar volume, and optical energy band gap of these glasses have been measured. The refractive index, molar refraction and polarizability of oxide ion have been estimated by using Lorentz–Lorentz relations. The optical absorption spectra of these glasses were revealed that fundamental absorption edge shifts to higher wavelengths as the content of Sm_2O_3 increases. The refractive index, optical energy band gap and Urbach energy had been calculated and explained.

(Received August 12, 2014; Accepted October 31, 2014)

Keywords: Borotellurite glass; optical band gap; Optical absorption coefficient; Fourier Transform Infrared Analysis (FTIR)

1. Introduction

The optical research on rare earth doped glasses draws much attention due to their wide applications in optical areas such as optical switches for laser and sensors and optical communications. The most important concerns in rare earth doped glasses are to define the dopant effect to the host materials.

Glasses have some unique properties such as high hardness and transparency at room temperature, along with sufficient strength and excellent corrosion resistance. Due to potential applications in various engineering and technological fields, the study of the properties of glasses is of great significance. Glassy materials have acknowledged advantages, like physical isotropy, the absence of grain boundaries, continuously variable composition they are practical to use for optical applications[1].

Tellurite glasses are very promising materials for laser and non-linear applications in optics, due to some of their important characteristic features, such as high refractive index, low phonon maxima and low melting point [2]. TeO_2 is known as a conditional glass former, as it needs a modifier in order to form the glassy state easily. The formation of glass on two glass formers such as borate glass and tellurite glass is of both scientific and practical interests[3]. This may lead to the formation of new structural units [4]. Tellurite glasses continue to intrigue both academic and industry researchers not only because of their technical applications, but also owing to a fundamental interest in understanding their microscopic mechanisms[5].

Borate oxide is one of the best materials which help to solidify the glass and enhance the glass quality with amelioration in transparency, refractive index and rare earth ion solubility and hardness. The borate matrix possesses well defined gathering of BO_3 triangles and BO_4 tetrahedra to form stable borate groups such as diborate, triborate and tetraborate[6]. Participation of zinc oxide in the glass formation creates low rates of crystallization, decreases the melting point and

* Corresponding author: halimah@science.upm.edu.my

increases the glass forming ability. It has been reported that [7] the effect of zinc oxide decreases the optical energy gap and increase the refractive index. Zinc oxide can occupy both network forming and network modifying positions in the borate network glasses and as a result, the physical properties of such glasses exhibit discontinuous changes, when the structural role of the cation changes [8].

Sailaja et al (2013) reported that the rare earth ions, Samarium (Sm) can be used as a dopant in different crystal hosts and also glass hosts for intense emissions in the visible region [9]. Especially, reddish orange emission region from Sm-doped materials possesses strong luminescence intensity, large stimulated emission cross section, and high quantum efficiency, which could be suitable for laser applications. Furthermore, Sm^{3+} ions are the important luminescent activators which are useful in characterizing the fluorescence properties because its $^4\text{G}_{5/2}$ level shows relatively high quantum efficiency [9].

2. Experimental

The glass sample was prepared by using the melt quenching method. The composition of zinc-borotellurite glass doped samarium $\{[(\text{TeO}_2)_{0.7}(\text{B}_2\text{O}_3)_{0.3}]_{0.7}[\text{ZnO}]_{0.3}\}_{1-x}\{\text{Sm}_2\text{O}_3\}_x$. For $x=0, 0.005, 0.01, 0.02, 0.03, 0.04, 0.05$ mol % were fabricated from Aesar grade tellurium (IV) oxide (TeO_2), (99.99% metals basis), zinc oxide (ZnO), (99.99%, metals basis), boron oxide B_2O_3 , (98.5%, metals basis) and samarium (III)oxide (Sm_2O_3), (99.9%, Reacton). The chemicals powder of $\text{TeO}_2, \text{B}_2\text{O}_3, \text{ZnO}$ and Sm_2O_3 were prepared at appropriate amount. The chemical powder of $\text{TeO}_2, \text{B}_2\text{O}_3, \text{ZnO}$ and Sm_2O_3 were weighed by using a digital weighing machine with accuracy of $\pm 0.0001\text{g}$ and mixed together thoroughly. The mixtures in alumina crucible were then put in electric furnace and preheat it at 400°C for 1 hour as to remove water content in the mixture.

After pre-heated process, the crucible was transferred to the second furnace at 900°C for a period of 2 hours. During the heating process, the cylindrical stainless steel was put in the first furnace at 400°C for a period of 1 hour. After 2 hours, the molten liquid was quenched rapidly into cylindrical stainless steel split mould which had been pre-heated at 400°C . The sample was immediately transferred to annealing process held at 400°C for a period of 1 hour and the furnace was turned off.

After annealing process, the glass sample was formed. The glass sample was cut at a thickness of about 2 mm by using low speed saw machine for the required measurements by using Isomet Buehler low speed saw machine. The sample was polished with various types of sand papers, 1500 grid, 1200 grid and 1000 grid to obtain flat and smooth surface.

The density of glass sample was measured at room temperature by using the Archimedes principle and distilled water was used as the immersion liquid. The weight of glass sample in the air and distilled water was weighed by using a digital weighing machine with accuracy of $\pm 0.0001\text{g}$. The corresponding molar volumes (V_m) were calculated by using the formula:

$$V_m = \frac{MW_t}{\rho} \quad (1)$$

Where M is the molecular weight and ρ is the density of glass samples.

The optical properties such as refractive index (n) will be determined by using EL X-02C high precision ellipsometer. Refractive index of these glasses is calculated by using the relation, which is proposed by Dimitrov and Sakka (1996).

$$\frac{n^2-1}{n^2+2} = 1 - \sqrt{\frac{E_g}{20}} \quad (2)$$

Where E_g the energy band gap. The structure of the glass was investigated using X-ray diffraction (XRD) and Fourier transforms infrared spectroscopy (FTIR). The optical absorption of the glass samples was measured by using UV-Visible spectroscopy Shimadzu UV-1650PC with the wavelength within the range of 200 nm to 1000 nm. The prepared glass samples were also grounded

into powder form for X-ray diffraction measurement by using X'pert Pro Panalytical Philips. The optical absorption coefficient $\alpha(\nu)$ was calculated for each sample by using the relation:

$$\alpha(\nu) = 2.303(A/d) \quad (3)$$

Where A denotes the absorbance and d indicates the thickness of the glass samples. Optical band gap energies (E_g) are calculated by the extrapolation of the linear region to meet $h\nu$ axis at $(\alpha h\nu)^{1/2} = 0$.

The molar refraction (R_M) was calculated by using the relation

$$\frac{n^2-1}{n^2+2} \left(\frac{M}{\rho}\right) = R_M \quad (4)$$

Where M is the molecular weight, ρ is the density of glass samples and n is the refractive index. The polarizabilities of these glasses have been estimated by using the Lorentz-Lorentz [10] relation

$$\frac{n^2-1}{n^2+2} (V_m) = \frac{4}{3} \pi N \alpha_e \quad (5)$$

Where V_m is the molar volume, N is the Avogadro number and α_e is the polarizability.

3. Results and discussion

3.1 Density and Molar volume

Density is an effective tool to explore the degree of structural compactness [11], modification of the geometrical configurations of the glass network, change in coordination and the variation of dimensions of the interstitial holes [3]. Furthermore; density was used in calculation of several important properties such as refractive index, elastic properties and thermal conductivity [12].

The calculated data of density are tabulated and shown in Table 1. It can be seen from Figure 1 that the density increases with an increase content of Sm_2O_3 . Eraiah et al (2006) proposed that the addition of a small amount of Sm_2O_3 into the glass network may resist the creation of non-bridging oxygen [12]. This will result the density to increase. The increasing trend of the density is due to the addition of modifier oxide which breaks up the Te-O-Te linkage [12], and increase the free space in the glass network [26]. It is known that the atomic mass of samarium (atomic mass of $Z_{\text{Sm}} = 150.36 \text{ gmol}^{-1}$) is greater than the atomic mass of tellurite ($Z_{\text{Te}} = 127.6 \text{ gmol}^{-1}$). The greater number of atomic mass in samarium compared to tellurite will give rise to the density in the glass system [15].

Table 1: Density and molar volume of samarium doped zinc borotellurite glass system

Samples	Density (kg/m^3)	Molar Volume (m^3/mol)
0.00	3.693	31.689
0.005	3.720	31.857
0.010	3.728	32.067
0.020	3.794	32.118
0.030	3.817	32.530
0.040	3.951	32.010
0.050	4.285	30.057

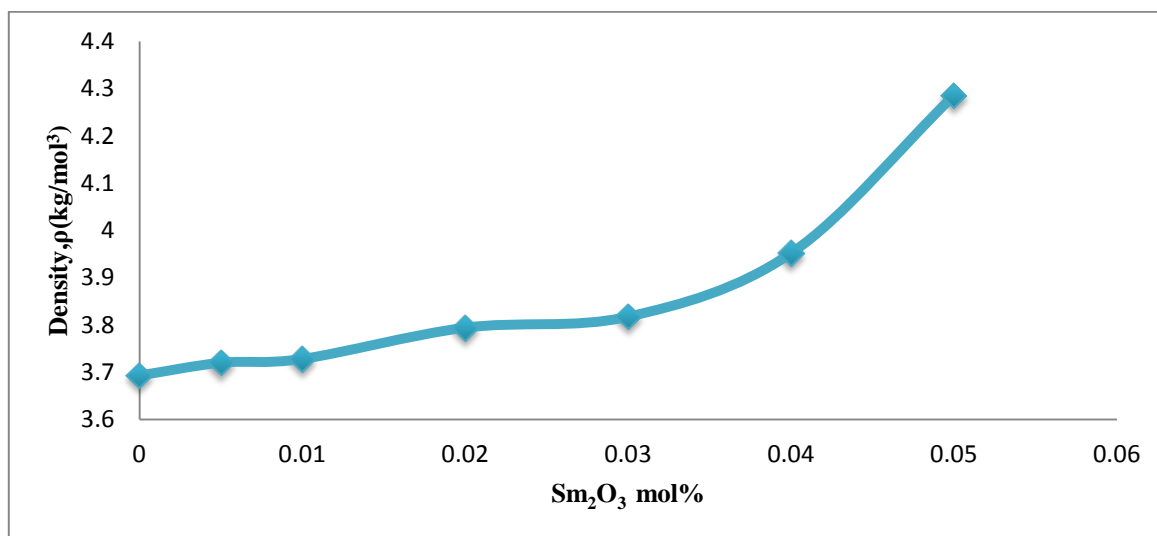


Fig. 1. Variation of density vs Sm₂O₃(mol%)

The molar volume data of the prepared glass samples are listed in Table 1. It is observed from Figure 2 that the molar volume increases with an increase in the content of samarium. This is due to the larger values of atomic radii and bond length of TeO₂ compared to ZnO [7]. Another possibility is that the ionic radii of samarium ($r = 185$ pm) is larger than tellurite ($r = 140$ pm) which results in the formation of excess free volume [15]. The existence of ZnO in the glass network results in the oxygen packing density to increase which squeezes the structure of the glass samples. The molar volume of the network increases with higher amounts of dopant. It is expected that the substitution of boron atoms by RE ions with bigger radii, such as samarium will result in an expansion of the rigid glass structure [27]. Moreover, the dopant ions break the bonds on the network, promoting the formation of non-bridging oxygens (NBOs-O), thus, resulting in a loosely packed structure [28]. It can be seen from Figure 2 that the molar volume decreases at 4% and 5% mol concentration of samarium which may be due to the dual nature of zinc oxide. Another possibility is that the atoms are more tightly packed, resulting in a denser glass [26].

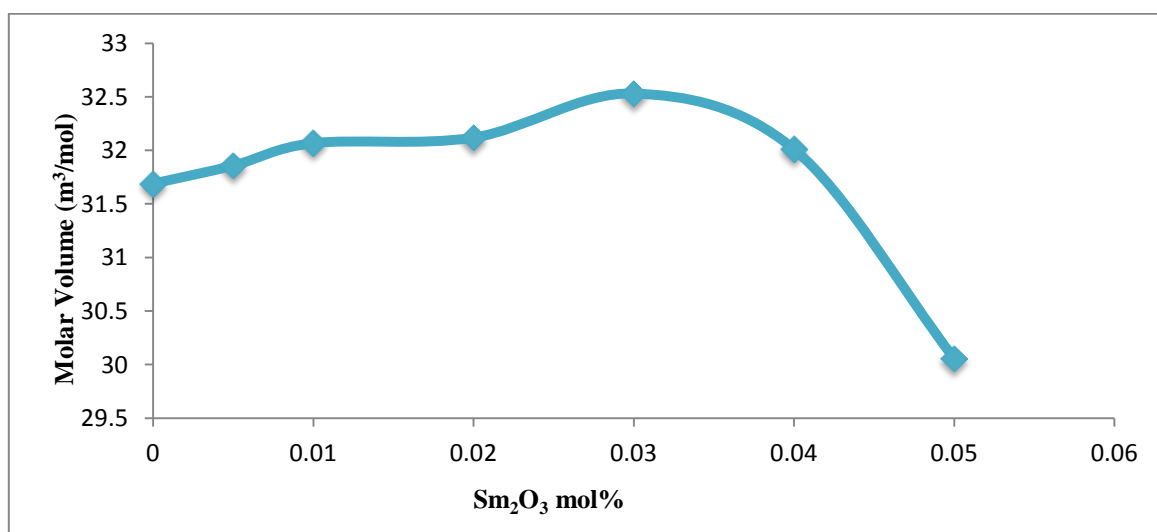


Fig. 2. Variation of molar volume vs Sm₂O₃ mol%

3.2 X-ray Diffraction Analysis (XRD) and Fourier Transform Infrared Analysis (FTIR)

The XRD analysis was used to confirm the amorphous or crystalline state of the materials. The X-ray diffraction pattern of samarium doped zinc borotellurite glasses was recorded in the range of $10^{\circ} \leq \theta \leq 80^{\circ}$. The results show that the XRD pattern of samarium doped zinc borotellurite glass exhibit broad diffusion at lower scattering angles indicating the presence of long range structural disorder which is the characteristic of an amorphous nature as shown in Figure 3.

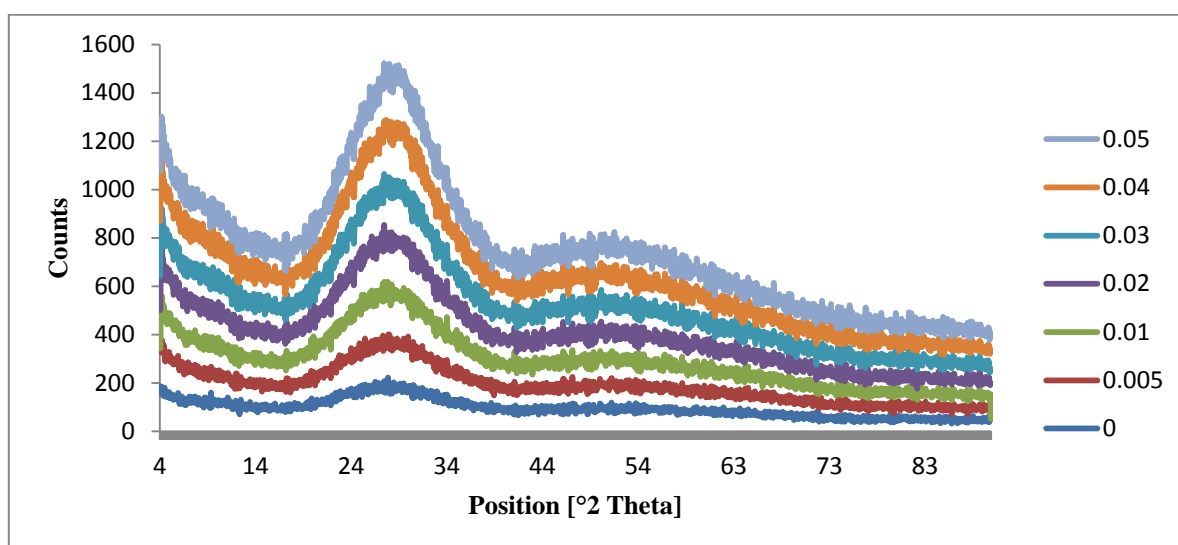


Fig. 3. XRD patterns with different concentration of samarium doped glass samples

Table 2. Assignment of infrared transmission bands of samarium doped glass sample

No.	0	0.005	0.01	0.02	0.03	0.04	0.05	*ASSIGNMENT
1	1342	1346	1346	1346	1346	1346	1346	Trigonal B-O bond stretching vibrations in isolated trigonal BO ₃ units [13].
2	1229	1239	1239	1239	1239	1239	1239	Trigonal B-O bond stretching vibrations of BO ₃ units from boroxyl rings[13].
3	1017	-	-	-	-	-	-	B-O bond stretching vibrations in BO ₄ tetrahedra from tri-, tetra-and penta-borate groups[14].
4	671	671	660-671	660	660	667	660	TeO ₃ group are exists in all tellurite containing glass[13].
5	-	-	-	-	-	-	-	ZnO participate in the glass network with ZnO ₄ structural units and alternate TeO ₄ units [13].

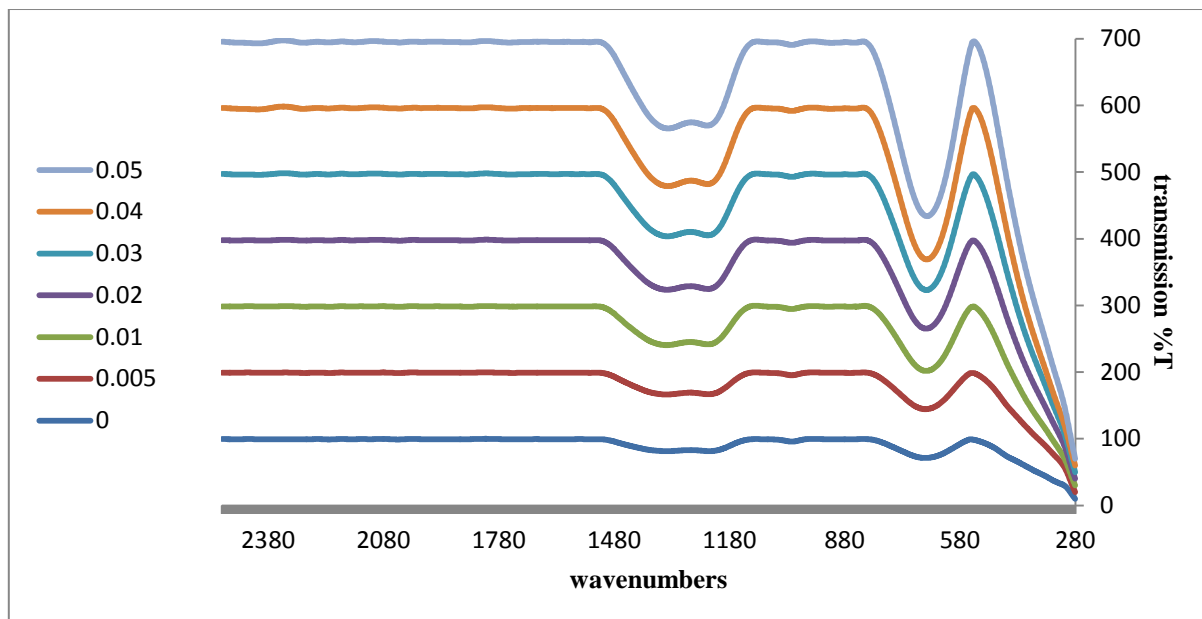


Fig. 4: FTIR spectra of zinc oxide, boron oxide, tellurite oxide, samarium oxide and $\{[(TeO_2)_{0.7}(B_2O_3)_{0.3}]_{0.7}[ZnO]_{0.3}\}_{1-x}\{Sm_2O_3\}_x$ glass system

The FTIR spectroscopy is an analysis method which offers structural studies to explore the fundamental and functional fractions in crystalline and non-crystalline matrices. The transmission spectra of the prepared glass samples are recorded in Figure 4 with different composition of samarium oxide. The observed broad bands are due to a combination of the higher degeneracy of vibrational states, thermal broadening of the lattice dispersion and mechanical scattering of the powdered samples and the corresponding band assignments [15].

The FTIR spectra of the prepared glass samples are recorded in the range of 300 – 4000 cm^{-1} as shown in Figure 4. It can be seen that the spectra consists of several peaks specifying its local structure [15]. The peak positions and their assignments are presented in Table 2. The transmission spectra of the glass structure consist of three extensive absorption bands; 660-671 cm^{-1} , 1017 – 1239 cm^{-1} and 1342 – 1346 cm^{-1} .

Tellurite oxide consists of two categories of structural configuration components i.e., trigonal bipyramid TeO_4 and trigonal pyramid TeO_3 . The characteristic of pure TeO_2 glass was centered at 640 cm^{-1} . The absorption band at 600 – 700 cm^{-1} was assigned by stretching vibrations of Te-O bonds in trigonal bipyramid, TeO_4 and trigonal pyramid, TeO_3 . Stretching vibrations of TeO_3 group possess higher frequency location than TeO_4 group. The first group of band formed around 600 – 650 cm^{-1} is correspond to TeO_4 trigonal bipyramid and the second group of band observed around 650 – 700 cm^{-1} is due to the TeO_3 trigonal pyramid [6]. The band shift of these groups depends on the changes in the composition of the glass network [7]. The manifestation band at 660 – 680 cm^{-1} designates that TeO_3 group exists in all tellurite containing glass orders. It can be seen that the band of ZnO does not appear in the spectra which means the zinc lattice is completely broken down [15].

In the pure borate glass, B_2O_3 was centered at 806 cm^{-1} frequency which indicates the characteristic of boroxyl ring. This band vanishes during the glass constitution which means there is no boroxyl ring in the glass composition. In the meantime, the BO_3 and BO_4 become visible in the absorption spectra after the glass formation which is due to the replacement of boroxyl ring. The absorption spectra of the borate glass can be divided into three regions: (1) 600-800 cm^{-1} (bending vibrations of various borate arrangement B-O-B), (2) 800-1200 cm^{-1} (B-O stretching of tetrahedral BO_4 units), (3) 1200-1800 cm^{-1} (B-O stretching of trigonal BO_3 units) [15]. The observed spectra for the first group of band are at 1233 – 1253 cm^{-1} which corresponds to B-O (B) stretching vibrations of polymerized BO_3 groups. The second group of band was observed at 1327 – 1343 cm^{-1} which associated with the trigonal B-O bond stretching vibrations in isolated trigonal BO_3 units. In addition, the absorption band positioned at 1200 – 1253 cm^{-1} is assigned to the

trigonal B-O bond stretching vibrations of BO_3 units from boroxyl groups. Meanwhile the absorption band positioned at $1388 - 1410 \text{ cm}^{-1}$ correspond to trigonal B-O bond stretching vibrations of BO_3 units from varied types of borate groups[15]. The absorption spectrum of samarium disappeared during the glass formation which may be due to the low concentration of samarium could not be detected by the device.

3.3 Optical absorption ,Optical band gap and Urbach energy

The optical absorption spectra of $\{[(\text{TeO}_2)_{0.7}(\text{B}_2\text{O}_3)_{0.3}]_{0.7} [\text{ZnO}]_{0.3}\}_{1-x} \{\text{Sm}_2\text{O}_3\}_x$ are shown in Figure 5. It can be seen that there are absent of any sharp absorption edges, which indicates the characteristic of the glassy state[16]. The absorption edge is affected by the oxygen bond strength in the glass system. The obtained data correspond to the change of the oxygen bond strength in the glass system[15]. It is also observed in the Figure 5 that the fundamental absorption edge shifts to higher wavelengths as the concentration of Sm_2O_3 increases. This may be due to the lower rigidity of the glass system resulting from higher Sm_2O_3 content[16].

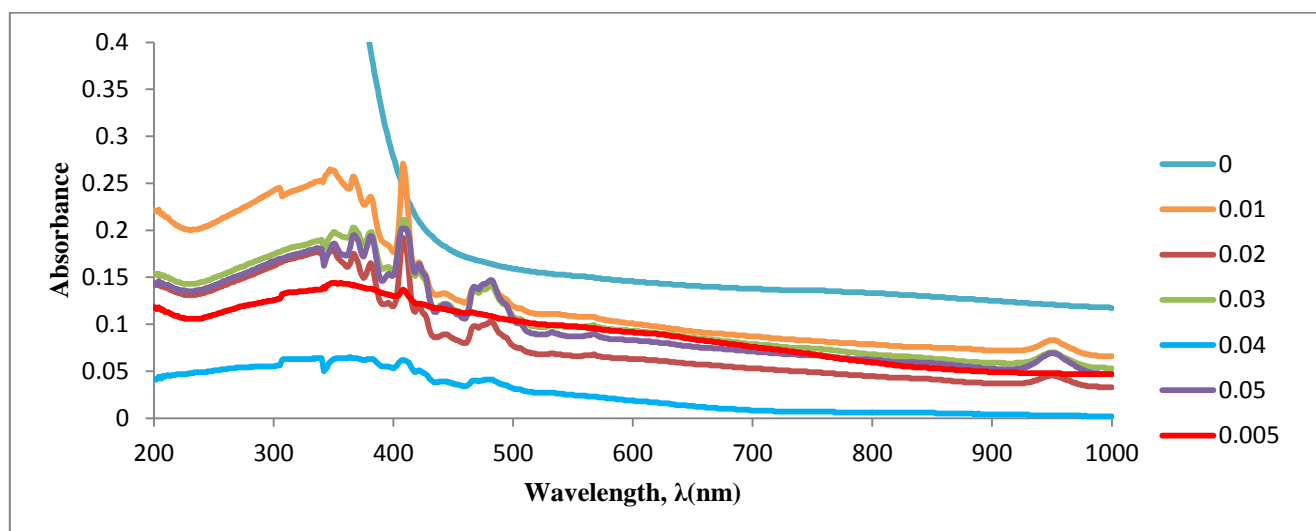


Fig. 5: Optical absorbance spectra for samarium doped glasses $\{[(\text{TeO}_2)_{0.7}(\text{B}_2\text{O}_3)_{0.3}]_{0.7} [\text{ZnO}]_{0.3}\}_{1-x} \{\text{Sm}_2\text{O}_3\}_x$

Optical absorption is an important parameter to investigate the optically induced transition and to determine the structural properties and optical band gap energy [15]. Mott and Davis proposed the relation between absorption coefficient and photon energy to calculate indirect and direct transitions occurring in a band gap [17]. The photon energy can be calculated by using the following equation:

$$\hbar\omega = \frac{h}{2\pi}(2\pi f) = hf = \frac{hc}{\lambda} \quad (6)$$

Where: $c = 2.9979 \times 10^8 \text{ (m/s)}$ and $\hbar = 4.14 \times 10^{-15} \text{ (eVs)}$

The absorption coefficient $\alpha(\omega)$ as a function of photon energy $\hbar\omega$ for direct and indirect optical transition as proposed by Mott and Davis is given by

$$\alpha(\omega) = \frac{B(\hbar\omega - E_{\text{opt}})^n}{\hbar\omega} \quad (7)$$

Where B is a constant related to the extent of the band tailing. $n=2$ for indirect transition and $n=1/2$ for allowed direct transitions. E_{opt} is the optical energy gap between the valence band and the conduction band. In both cases, electromagnetic waves interact with the electrons in the valence band, which are raised across the fundamental gap to the conduction band [18].

The absorption coefficients, $\alpha(\nu)$, are determined near the absorption edge at different photon energies for all glass samples [5]. The plotted graph of $(\alpha\hbar\omega)^2$ and $(\alpha\hbar\omega)^{1/2}$ versus photon energy ($\hbar\omega$) are correspond to direct and indirect transitions as shown in Figure 6a and 6b respectively. In amorphous material, the plot of $(\alpha\hbar\omega)^{1/2}$ versus $\hbar\omega$ was plotted for direct band gap to determine whether optical data on the glass samples are better fit to direct or indirect band gap [5]. The slope of the graph was used to find the band gap energy for direct and indirect transitions. The data of indirect and direct band gap as a function of photon energy for $\{[(\text{TeO}_2)_{0.7}(\text{B}_2\text{O}_3)_{0.3}]_{0.7}[\text{ZnO}]_{0.3}\}_{1-x}\{\text{Sm}_2\text{O}_3\}_x$ glass system is tabulated in Table 3 and shown in Figure 7a and Figure 7b respectively. It is observed that the values of the direct band gap are larger than the corresponding values of the indirect band gap. The indirect band gap is found to be in the range of 2.529 to 2.846 eV. It can be seen from the Figure 7a, 7b that the band gap decreases at 0.005 mol % and 0.04 mol % and increases at 0.01 mol % and 0.05 mol % along with concentration of samarium. The decreasing value of E_g at 0.005 and 0.04 mol % are may be due to the variation of density as well as the increasing number of non-bridging oxygens which alter the glass structure [5]. Another possibility could be that at high dopant concentrations, the broadening of the impurity band and the formation of band tails on the edges of the conduction and valence bands would lead to a reduction in E_g as in semiconductors [19]. The existence of trivalent electrons of samarium ions affects the structure of the glass system by increasing number of free electrons which leads to decreasing number of band gap energy. The change in band gap is due to the shifts of the valence and conduction band from each other [15].

Table 3: Indirect optical band gap (E_{opt}^1), Direct optical band gap (E_{opt}^2) and Urbach energy (ΔE) of samarium doped glass samples

Samples	Indirect band gap, E_{opt}^1 (eV)	Direct band gap, E_{opt}^2 (eV)	Urbach energy, ΔE (eV)
0.000	2.780	2.845	0.689
0.005	2.528	2.804	0.579
0.010	2.898	2.970	0.630
0.020	2.921	2.970	0.662
0.030	2.851	2.951	0.689
0.040	2.782	2.920	0.513
0.050	2.845	2.943	0.660

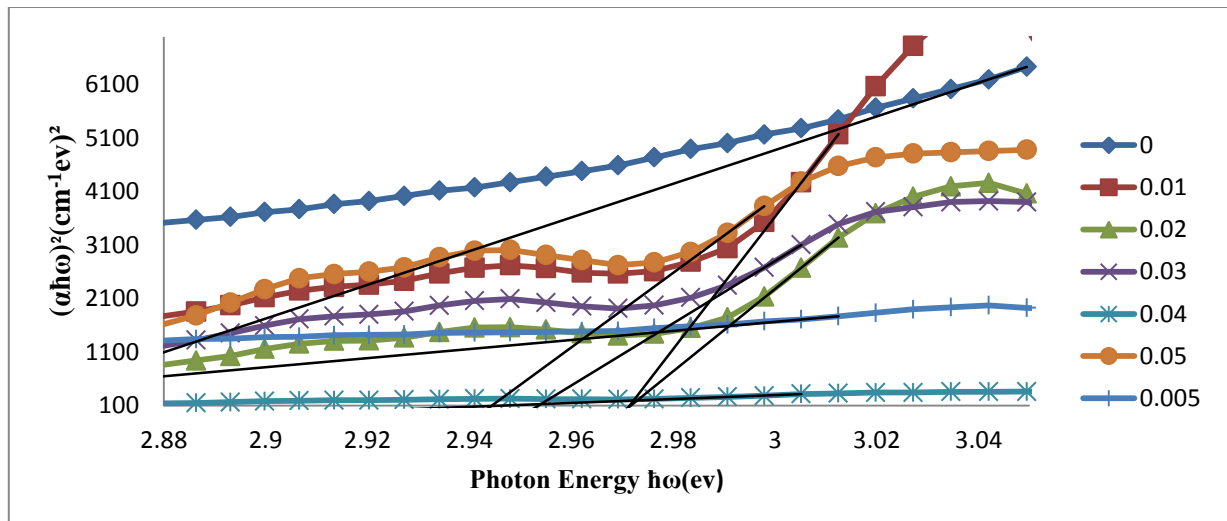


Fig. 6a: Plot of $(\alpha\hbar\omega)^2$ against photon energy $\hbar\omega$ of samarium doped glass samples for direct band gap measurement

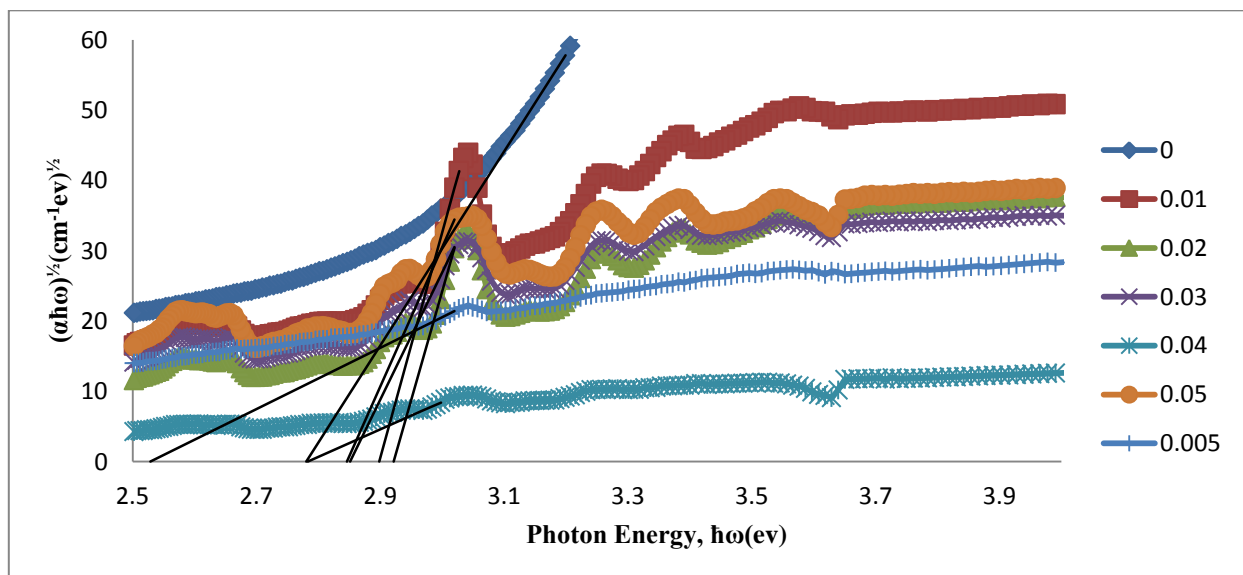


Fig. 6b: Plot of $(\alpha\hbar\omega)^{1/2}$ against photon energy $\hbar\omega$ of samarium doped glass samples for indirect band gap measurement

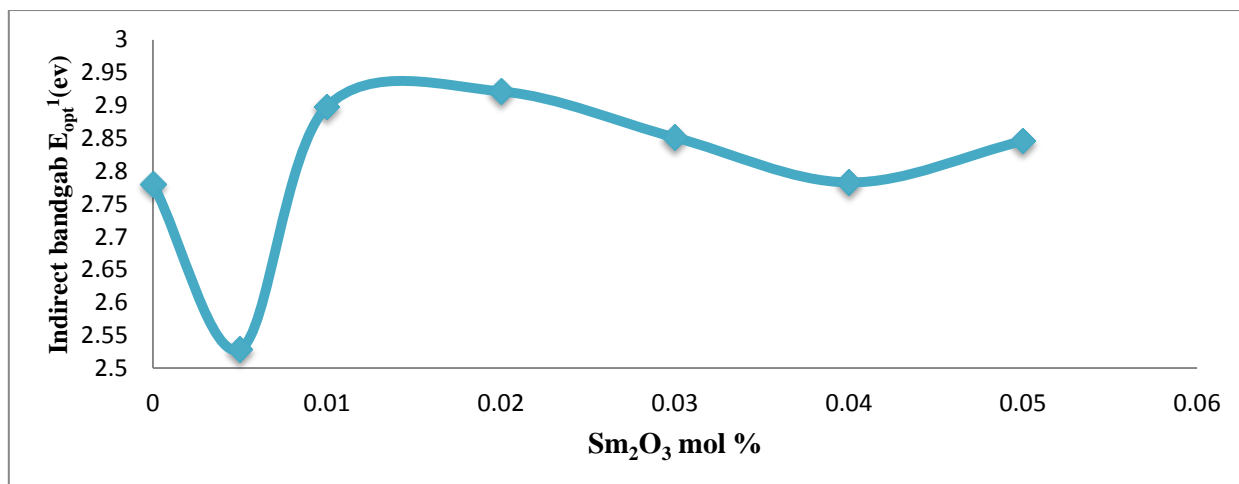


Fig. 7a: Variation of indirect optical band gap with glass composition for indirect transition for samarium doped glass samples

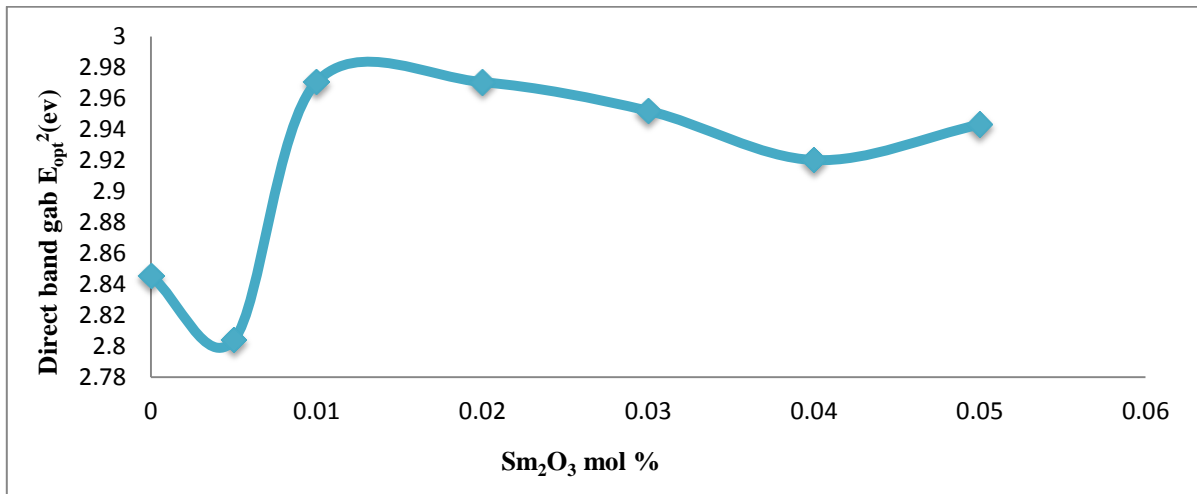


Fig. 7b: Variation of direct optical band gap with glass composition for direct transition for samarium doped glass samples

Urbach energy (ΔE) gives information regarding on the character of disorder in the amorphous materials[15].The values of the Urbach energy ΔE are calculated by taking the reciprocals of the slopes of the linear portion of the $\ln\alpha(\nu)$ versus $\hbar\omega$ curves in the lower photon energy regions[16]as showed in Figure 8. It is given by [20]:

$$\alpha(\nu)=\beta\exp\left(\frac{\hbar\nu}{\Delta E}\right) \quad (8)$$

where β is a constant, \hbar is the Plank constant, ν is the photon frequency and ΔE is the Urbach energy which corresponds to the width of localized states which is used to characterize the degree of disorderness in the amorphous and crystalline materials [6,15].These values are given in Table 3, and showed in Figure 9.

The trend of the Urbach energy values is shown to be non-linear. It is known that materials which possess a large value of Urbach energy have higher tendency to convert the weak bonds into defects [15]. Hence, the trend of increasing in the Urbach energy with Sm₂O₃ content confirms that the number of defects also increases[16].This is probably due to the increase in the TeO₄ pyramids as the content of Sm₂O₃ oxide increase. The presence of TeO₄ pyramids results the structure to become less stable and lower connectivity in the glass network[15].Halimah *et al.*(2005)proposed that the addition of TeO₂ to the glass system shows a reduction in the optical band gap as well as Urbach tails with the densification of the glass network[3].

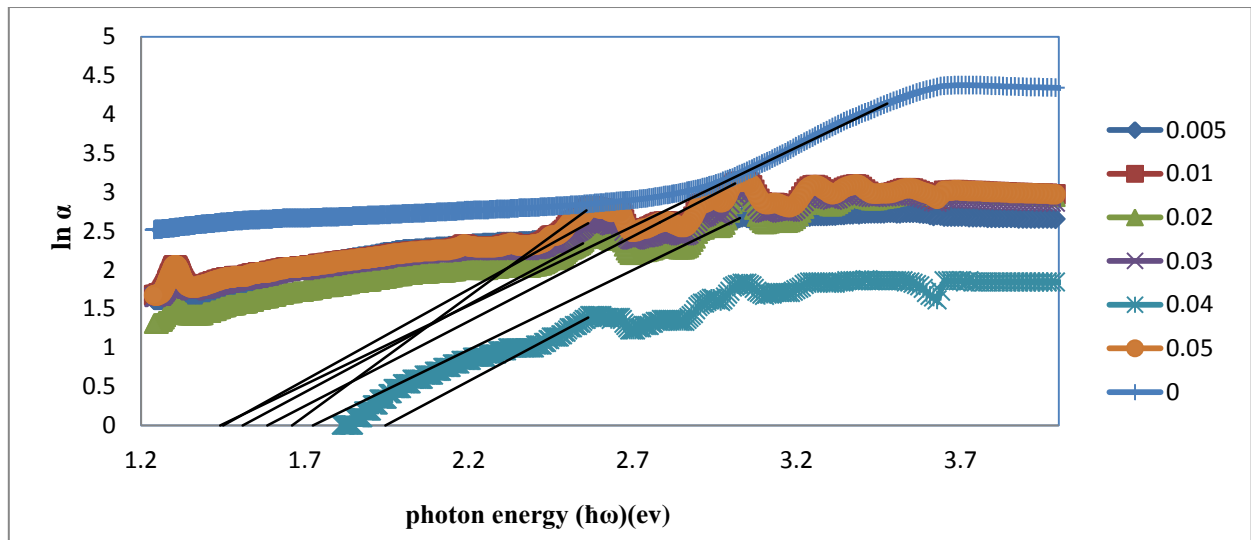


Fig. 8: Variation of $\ln(\alpha)$ with photon energy $\hbar\omega$ (eV) for different Sm_2O_3 mol%

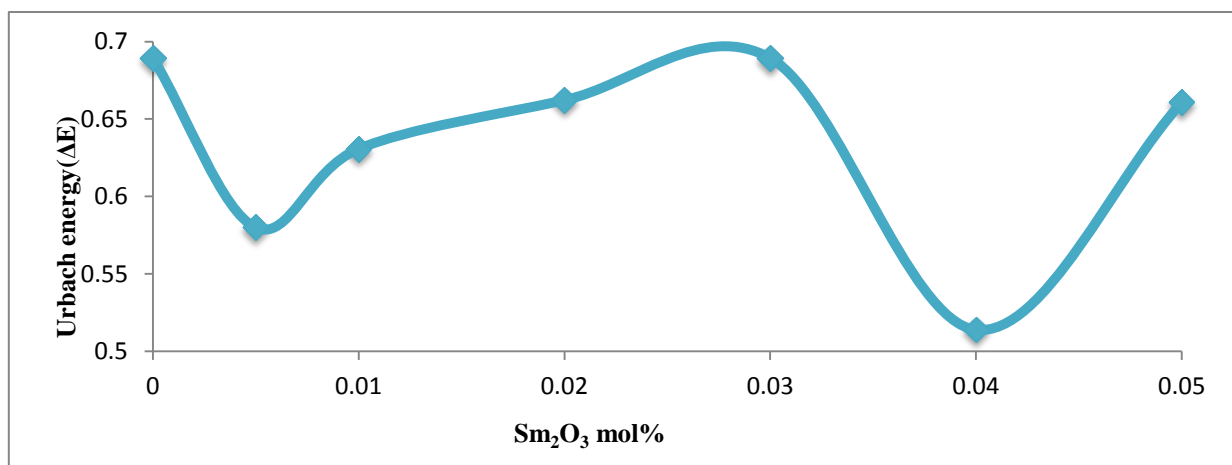


Fig. 9: Variation of Urbach energy (ΔE) vs Sm_2O_3 mol%

3.4 Refractive index (n), molar refraction (R_M) and polarizability (a_e)

Refractive index is one of the most significant properties in optical glasses. Therefore, a large number of researchers have carried out investigations to ascertain the relation between refractive index and glass composition [21].

The main role of polarizability is to govern the nonlinear response of the materials. The optical non-linearity is caused by the electronic polarization of the materials upon exposure to intense light beams [12]. Polarizability is related to many macro and microscopic physical and chemical properties such as optical UV absorption of metal ions, electro-optical effect etc [22].

Table (4): Refractive index, molar refraction and polarizability of samarium doped zinc borotellurite glass system

Samples	Refractive index(n)	Molar refraction (R_M) (cm^3)	Polarizability(α_e) ($\times 10^{-24}$) (cm^3)
0.000	1.871	14.412	5.716
0.005	1.893	14.749	5.849
0.010	1.974	15.752	6.248
0.020	1.873	14.633	5.804
0.030	1.968	15.923	6.315
0.040	2.030	16.327	6.487
0.050	2.005	15.080	5.981

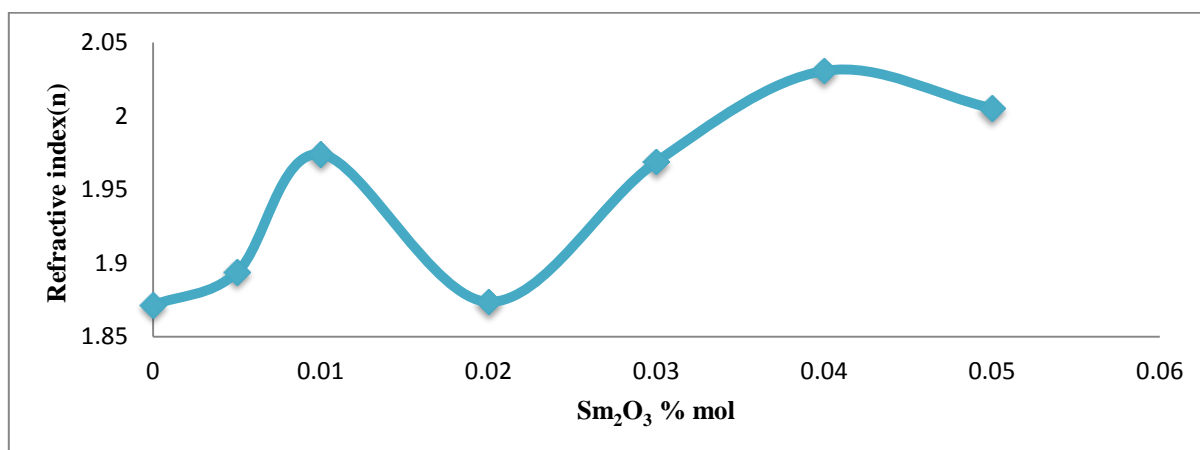


Fig. 10: Variation of refractive index vs Sm_2O_3 mol%

Refractive index (n) and molar refraction (R_M) depend upon the polarizability and density of materials. The more polarizable the outer electrons, the higher the refractive index and molar refraction [12].

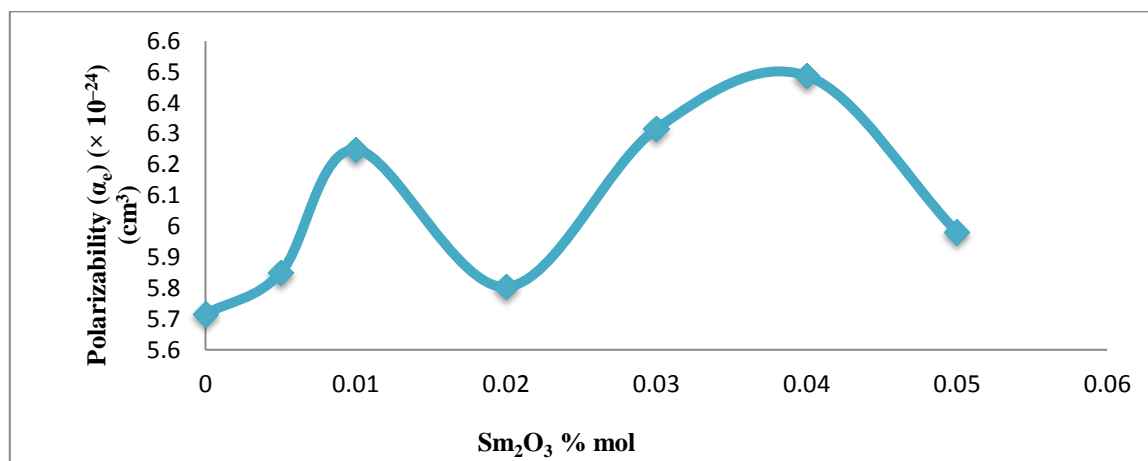


Fig. 11: Variation of polarizability vs Sm_2O_3 mol%

Refractive index (n), polarizability (α_e) and molar refraction (R_M) data for samarium doped glass samples are listed in Table 4 and shown in Figure 10, 11 and 12 respectively. It can be seen from Figure 10 that the refractive index increases with increasing concentration of Sm_2O_3 at 0.01 mol% and 0.04 mol%. The refractive index suddenly decreases gradually at 0.02 mol% and 0.05 mol% of Sm_2O_3 . The same trend has been observed in the case of molar refraction (R_M) and polarizability (α_e). The trend of increasing the value of (n), (R_M) and (α_e) is due to the substitution of ZnO oxides into TeO_2 which results the bridging Te-O-Te to be broken and increases the non-bridging Te-O-Zn^{2+} [23]. The non-bridging oxygen (NBO) bonds have a much higher ionic character and much lower in bond energies. Consequently, the NBO bonds possess higher polarizability and cation refraction than bridging oxygen. The relationship between polarizability and refractive index is a direct proportional behavior which means higher polarizability results in higher refractive index of the glass system [15]. The variation of (n) and (α_e) at 0.02 mol% and 0.05 mol% Sm_2O_3 may be due to the dual nature of ZnO which acts as network modifier and it may occupy the network former position [24]. Another possibility is that the substitution of cations into TeO_2 network induces a structural variation from $(\text{TeO}_4)^4-$ to $(\text{TeO}_3)^{2-}$ entities through an intermediate asymmetric structure [25]. This leads to a significant change in the optical properties [5].

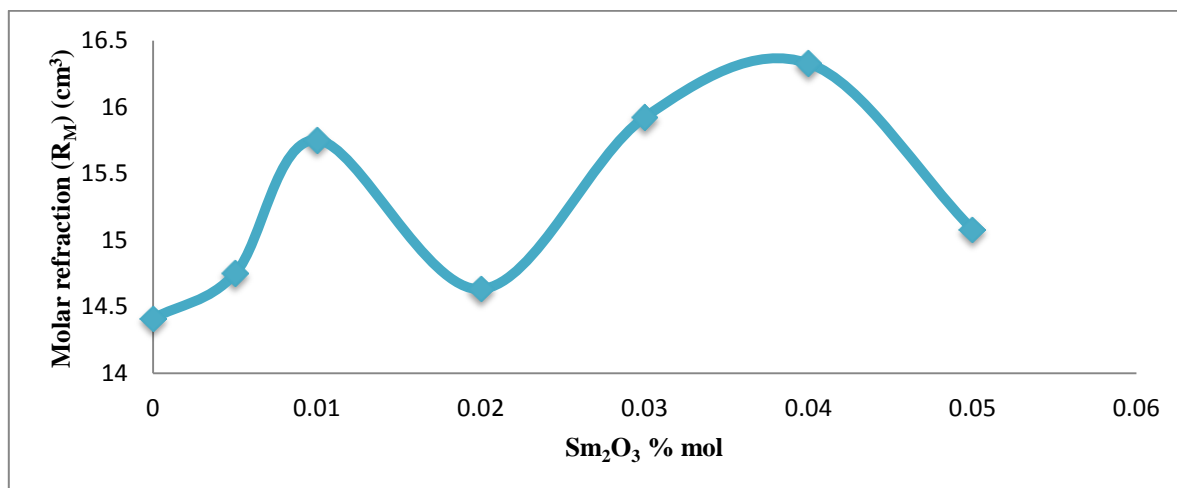


Fig. 12: Variation of molar refraction vs Sm_2O_3 mol%

4. Conclusions

Samarium doped zinc-borotellurite glasses have been studied and investigated. The density of the prepared glass samples is found to be increased with an increasing content of samarium which is due to the formation of non-bridging oxygen. The molar volume of these glasses increases up to 0.03 mol% of Sm_2O_3 which is due to the large value of ionic radii and bond length of Sm_2O_3 compared to TeO_2 and increasing in oxygen packing density which results the structure becomes more compact. The XRD analysis confirmed that all the glass samples are amorphous. The FTIR analysis consists of several bands which indicate the characteristic of Te-O and B-O vibrational groups. The optical absorption spectra of these glasses revealed that fundamental absorption edge shifts to longer wavelength as the content of Sm_2O_3 increases. The decreasing value of the band gap energy is due to the increasing number of non-bridging oxygen. The non-linear trend of refractive index and polarizability are due to the substitution of ZnO oxides which acts as a modifier and former at certain values of mol%. The Urbach energy is found to increase with increasing content of samarium. This is due to the increasing number of TeO_4 pyramids as the content of Sm_2O_3 oxide increases. The presence of TeO_4 pyramids results the structure to become less stable.

Acknowledgments

The authors appreciate the financial support for the work from the Ministry of Higher Education of Malaysia through Research University Grants RUGS(9411800).

References

- [1] C.M.Joseph,P.R. Binu, K. Shreekrishnakumar, *Materials Letters*, **50**, 251 (2001).
- [2] G. V.prakash, D.N. Rao A.K. Bhatnagar, *Soild state commun*, **119**, 39 (2001).
- [3] M. K. Halimah,W. M. Daud, H. A. A. Sidek, *Journal of Applied Sciences*, **2340**, 1546 (2005).
- [4] V. Rajendran,N. Palaniveluand B. K. Chaudhuri, *Journal of NoncrystallineSolids*, **320**(1), 195 (2003).
- [5] B. Eraiah, *Indian Academy of Sciences*, **33**(4), 391 (2010).
- [6] K. Maheshvaran, P. Veeran, K. Marimuthu, *Journal of solid state sciences*, **17**, 54 (2013).
- [7] P. G.Pavani, K. Sadhanaand V. C.Mouli, *Journal of Physica B*, **406**(6-7), 1242 (2011).
- [8] M. Farouk, A. Samir, F. Metawe, *Journal of non-crystalline solids*, **371**, 14 (2013).
- [9] S. Sailaja, C. N. Raju, C. A. Reddy, *Journal ofMolecular Structure*, **1038**, 29 (2013).
- [10] H. Rawson, *Amster-dam-Elsevier Scientific Pub*, **3**, 318 (1980).
- [11] M. R.Raddy, V. R. Kumar, N.Veeraiah, *Indian Journal of Pure and Applied Physics*, **33**, 48 (1995).
- [12] B. Eraiah, *Journal of Indian Academy of Sciences*, **29**(4), 375 (2006).
- [13] S. Rada, A. DeheleanandE. Culea, *Journal of non-crystalline solids*, **357**, 3070 (2011).
- [14] K. Maheshvarana, K. Linganna K. Marimuthuan, *Journal of Luminescence*, **131**, 2746 (2011).
- [15] M. N. Azlan, M. K. Halimah, S. Z. Shafinasand, W. M. Daud, *Journal of Nanomaterials*, **2013**, 1 (2013).
- [16] M. K. Halimah,W. M. Daud, H. A. A. SidekandA. W. Zaidan, *Materials Science- Poland*, **28**(1), 173 (2010).
- [17] H.Aboud., H. Wagiran I. Hossain, *Journal of materials letters*, **85**, 21 (2012).
- [18] N. Ahlawat, S. Sanghi, A. Agarwal, *Journal of Alloys and Compounds*, **480**, 516 (2009).
- [19] S. A. Aw, H. S. Tan C. K. Ong, *J. Phys.: Condens. Matter*, **3**, 8213 (1991).
- [20] M. D. Reza, M. R. Sahar, S. K. Ghosal, *Journal of molecular structure*, **1035**, 6 (2013).
- [21] R. El-Mallawany, *Journal of Applied Physics*, **72**, 1774 (1992).
- [22] V. Dimitrov S. Sakka, *Journal of Applied Physics*, **79**,1736 (1996).
- [23] B. Eraiah, G. Sudha, Bhat, *Journal of Physics and Chemistry of Solids*, **68**, 581 (2007).
- [24] M. Ganguly, M. H.Bhat, K. J. Rao, *Phys. Chem. Glasses*, **40**, 297 (1999).
- [25] S. Neov, V. Kozhukharov, I. Gerasimovaand B. Sidzhimov, *Journal ofphysics C: Soild state Physics*, **12**, 2475 (1979).
- [26] P. Damas, J. Coelho, G. Hungerford, N. S. Hussain, *Materials Research Bulletin*, **47**, 3489 (2012).
- [27] M. Subhadra, P. Kistaiah, *Physica B:of Condensed Matter*, **406**(8), 1501 (2011).
- [28] Y.B. Saddeek, L.A.E. Latif, *Physica B: Condensed Matter*, **348**(1), 475 (2004).